Int. J. Heat Mass Transfer. Vol. 24, pp. 541 544
Pergamon Press Ltd. 1981. Printed in Great Britain

0017-9310/81/0301-0541 $02.00/0

ON THE RELATION BETWEEN CRITICAL HEAT FLUX AND OUTLET FLOW PATTERN OF FORCED CONVECTION BOILING IN UNIFORMLY HEATED VERTICAL TUBES

Y. KATTO

Department of Mechanical Engineering, University of Tokyo,
Hongo, Bunkyo-ku, Tokyo, Japan

(*Received* 9 *April* 1980)

Abstract—For critical heat flux (CHF) of forced convection boiling in uniformly heated vertical tubes, the author recently proposed generalized correlation equations being classified into four characteristic CHF-regimes called L, H, N and HP. In the present paper, a study is made on the relation between the above-mentioned CHF-regimes and the flow patterns at the tube exit, by employing existing data of flow patterns for uniformly heated tubes.

NOMENCLATURE

d, I.D. of heated tubes [m];
G, mass velocity [$\mathrm{kg\,m^{-2}\,s^{-1}}$];
H_{fg}, latent heat of evaporation [$\mathrm{J\,kg^{-1}}$];
ΔH_i, enthalpy of inlet subcooling [$\mathrm{J\,kg^{-1}}$];
l, length of heated tube [m];
p, absolute pressure [bar];
q, heat flux [$\mathrm{W\,m^{-2}}$];
q_c, critical heat flux [$\mathrm{W\,m^{-2}}$];
T_i, inlet temperature [°C];
T_s, saturation temperature [°C].

Greek symbols

ρ_l, density of liquid [$\mathrm{kg\,m^{-3}}$];
ρ_v, density of vapor [$\mathrm{kg\,m^{-3}}$];
σ, surface tension [$\mathrm{N\,m^{-1}}$];
χ_{ex}, exit quality.

1. INTRODUCTION

ANALYZING experimental data of critical heat flux (CHF) of forced convection boiling in uniformly heated vertical tubes, the author [1–3] presented generalized correlation equations of CHF being classified into four characteristic regimes called L, H, N and HP. Then, it was followed by a study on generalized graphic representation of many existing CHF data [4], showing that the author's correlation equations of CHF are capable of outlining the general features of CHF concerned.

L-regime mentioned above is the regime that takes place when mass velocity G is low for fixed other conditions, whereas N-regime makes the appearance when G is very high; and H-regime is the intermediate one between L- and N-regime. On the other hand, HP-regime is a special one that replaces N-regime when the system pressure is extremely high. In addition, N-regime has a character distinguishing itself from the other three regimes by showing non-linear relationship between critical heat flux q_c and inlet subcooling enthalpy ΔH_i (cf. [1]).

Then, it is well known (cf. Collier [5] for example) that for uniformly heated channels, the onset of CHF condition can be assumed to occur first at the exit end of the channel. Therefore, relating to the study on the mechanism of CHF, it may not be useless to investigate the connection between characteristic CHF-regimes and flow patterns at the tube exit.

2. FLOW PATTERNS AT THE TUBE EXIT

Bergles and Suo [6] measured flow patterns of water/steam two-phase flow in uniformly heated vertical tubes, changing both the mass velocity G and the heat flux q under the conditions of pressure p = 34.5 bar (with three kinds of inlet temperature T_i = 121, 163 and 204°C against saturation temperature T_s = 241°C) and p = 69 bar (with three kinds of inlet temperature T_i = 149, 204 and 260°C against saturation temperature T_s = 283°C), internal diameter of heated tube d = 0.0102 m, and three kinds of length/diameter ratio of tube l/d = 60, 150 and 240. In the above study, classification of flow pattern was made by recording the variation of conductance between the tube wall and the tip of an electrical resistance probe inserted into the flow at the tube exit. As a result, four kinds of flow regimes called bubbly, slug, froth and spray annular, were classified to give flow regime maps, where flow pattern boundaries were represented in terms of the mass velocity G and the exit quality χ_{ex}.

For uniformly heated round tubes, the following equation holds via heat balance:

$$\frac{q}{GH_{fg}} = \frac{1}{4}\frac{d}{l}\left(\chi_{ex} + \frac{\Delta H_i}{H_{fg}}\right) \tag{1}$$

where H_{fg} is the latent heat of evaporation. Through this equation, therefore, the value of q/GH_{fg} is readily estimated at a point on the flow regime maps mentioned above (Figs. 6–8 in [6]), while the value of $\sigma\rho_l/G^2 l$ at the same point (where σ is the surface tension and ρ_l the density of liquid) can be determined from the experimental conditions. In other words, the

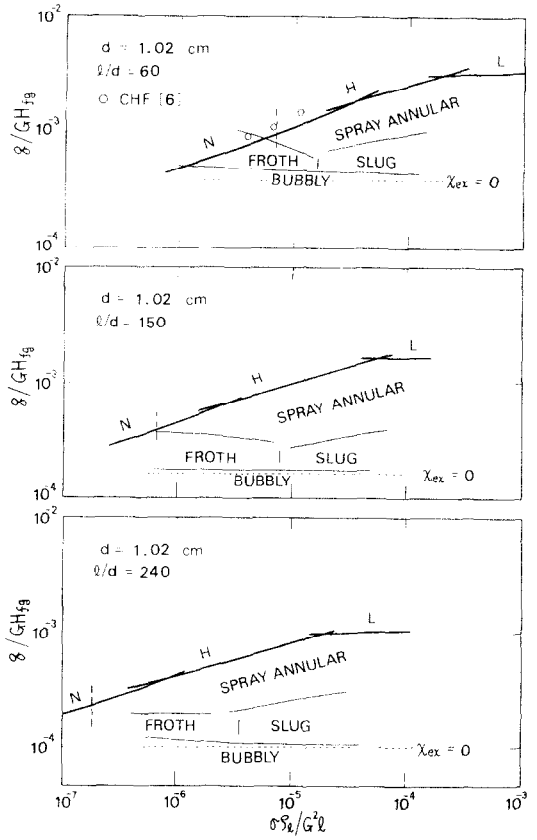

FIG. 1. Flow patterns at the tube exit (Bergles and Suo [6]) and characteristic CHF-regimes. Water, p = 34.5 bar, T_s = 241°C, T_i = 204°C ($\Delta H_i/H_{fg}$ = 0.0975).

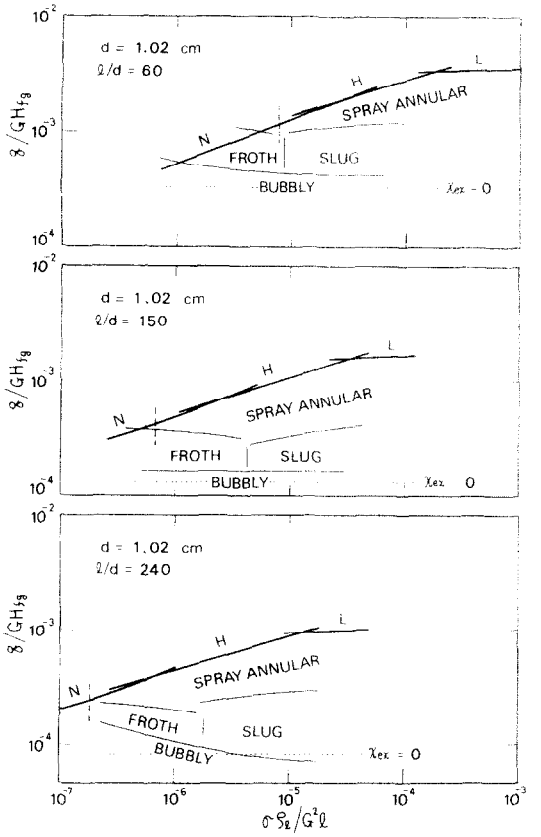

FIG. 2. Flow patterns at the tube exit (Bergles and Suo [6]) and characteristic CHF-regimes. Water, p = 69 bar, T_s = 283°C, T_i = 260°C ($\Delta H_i/H_{fg}$ = 0.0799).

flow regime map of G-χ_{ex} type obtained by Bergles and Suo can be transformed to the diagram of (q/GH_{fg})-$(\sigma\rho_l/G^2l)$ type, and typical results are shown in Fig. 1 for the case of T_i = 204°C at p = 34.5 bar, and in Fig. 2 for the case of T_i = 260°C at p = 69 bar. A horizontal dotted line in each diagram of Figs. 1 and 2 represents the value of heat flux q to generate $\chi_{ex} = 0$ at the tube exit; and three open circles plotted in the top diagram of Fig. 1 represent experimental data of CHF measured by Bergles and Suo.

On the other hand, Bennett *et al.* [7] made experiments with water under the condition of pressure p = 34.5 bar and 69 bar (inlet subcooling temperature $T_s - T_i \doteqdot 11$ to 17°C in both cases), internal diameter of heated tube d = 0.0126 m, and tube length l = 3.66 m. In this study, the flow pattern was detected by means of still and high-speed moving pictures of the two-phase flow emerging from the end of the uniformly heated vertical tube, complemented by X-ray photography of the flow in the heated tube, to give flow regime maps of G-χ_{ex} type (Fig. 5.7 for p = 34.5 bar and Fig. 5.8 for p = 69 bar in [7]).

Then, a diagram of (q/GH_{fg})-$(\sigma\rho_l/G^2l)$ type corresponding to the above flow regime map in case of 69 bar alone is shown in Fig. 3, for simplicity. A chain line in Fig. 3 is the experimental CHF line obtained by Bennett *et al.* It is noted that experimental conditions giving the result of Fig. 3 are close to those of the bottom diagram of Fig. 2, and it is a matter of no importance that the dotted line of $\chi_{ex} = 0$ in Fig. 3 is located lower than that in Fig. 2, because it only depends on the difference of inlet subcooling. In addition, according to the two reports [6, 7], it may be assumed that the froth flow in Fig. 2 and the wispy annular flow in Fig. 3 designate nearly a similar flow pattern, so that Figs. 2 and 3 are not so different from each other. The boundary between the froth and spray annular flow in the bottom diagram of Fig. 2 is different in position from the boundary between the wispy annular and annular flow in Fig. 3; but following Bergles and Suo, it may be presumed that the discrepancy is due in large part to the different detection techniques of flow pattern.

3. CHARACTERISTIC REGIMES OF CHF

Critical heat flux q_c for a flow with inlet subcooling enthalpy ΔH_i is now written as:

$$q_c = q_{co}\left(1 + K\frac{\Delta H_i}{H_{fg}}\right). \tag{2}$$

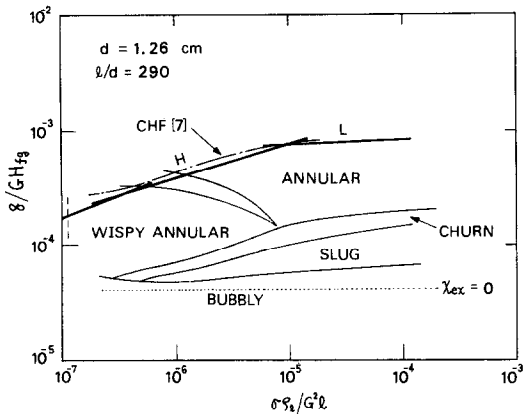

FIG. 3. Flow patterns at the tube exit (Bennett *et al.* [7]) and characteristic CHF-regimes. Water, $p = 69$ bar, $T_s = 283°C$, T_i (average) $= 269°C$ ($\Delta H_i/H_{fg} = 0.0476$).

Then, according to the author's preceding paper [4], q_{co} on the RHS of equation (2) is evaluated as follows:

L-regime*:

$$\frac{q_{co}}{GH_{fg}} = C\left(\frac{\sigma\rho_l}{G^2l}\right)^{0.043}\frac{1}{l/d} \tag{3}$$

where $C = 0.25$ for $l/d < 50$, $C = 0.34$ for $l/d > 150$, and C changes linearly from 0.25 to 0.34 with l/d for $l/d = 50$ to 150.

H- and N-regime:

$$\frac{q_{co}}{GH_{fg}} = 0.10\left(\frac{\rho_v}{\rho_l}\right)^{0.133}\left(\frac{\sigma\rho_l}{G^2l}\right)^{1/3}\frac{1}{1+0.0031\,l/d} \tag{4}$$

and

$$\frac{q_{co}}{GH_{fg}} = 0.098\left(\frac{\rho_v}{\rho_l}\right)^{0.133}\times\left(\frac{\sigma\rho_l}{G^2l}\right)^{0.433}\frac{(l/d)^{0.27}}{1+0.0031\,l/d} \tag{5}$$

where ρ_v is the density of vapor. The boundary between H- and N-regime is given by

$$\frac{\sigma\rho_l}{G^2l} = \left(\frac{0.77}{l/d}\right)^{2.70}. \tag{6}$$

Next, the author's previous paper [3] has shown that K on the RHS of equation (2) is derived theoretically from equations (3)–(5) by utilizing the linear relationships between q_c and ΔH_i as well as the concept of boiling length as follows:

L-regime: corresponding to equation (3),

$$K = \frac{1.043}{4C(\sigma\rho_l/G^2l)^{0.043}} \tag{7}$$

H-regime: corresponding to equation (4),

$$K = \frac{5}{6}\frac{0.0124 + d/l}{(\rho_v/\rho_l)^{0.133}(\sigma\rho_l/G^2l)^{1/3}} \tag{8}$$

and corresponding to equation (5),

$$K = 0.416\frac{(0.0221 + d/l)(d/l)^{0.27}}{(\rho_v/\rho_l)^{0.133}(\sigma\rho_l/G^2l)^{0.433}}. \tag{9}$$

For N-regime, the linear relationship between q_c and ΔH_i does not hold, so that the equation of evaluating K has not been determined. However, if it is limited to the range of small ΔH_i for N-regime near H-regime, equation (9) may probably be used approximately for predicting the effect of subcooling on CHF in N-regime without serious error. In the present paper, therefore, q_c in N-regime is estimated by this approximate means. Thick lines in Figs. 1–3 represent CHF thus estimated through equations (2)–(9), and the marks of L, H, and N indicate characteristic regimes of CHF, where the vertical broken line separating N-regime from H-regime is given by equation (6).

4. DISCUSSIONS

(i) It is noted in the top diagram of Fig. 1 that three open circles showing the data of CHF measured by Bergles and Suo have appeared near the prediction of CHF by the author's correlation equations, and it is also noted in Fig. 3 that the situation is quite the same for the experimental CHF line obtained by Bennett *et al.*

(ii) Through all the six diagrams of Figs. 1 and 2, it may be assumed approximately that the flow pattern at the tube exit is spray annular when CHF takes place in L- and H-regime, whereas it is froth (or bubbly) when CHF takes place in N-regime. As for Fig. 3, the similar situation as above may probably be assumed in a rough sense at least (see comments on Fig. 3 described in Section 3).

(iii) The result of the preceding item (ii) suggests that the flow pattern near the tube exit is almost identical for both L- and H-regime. Therefore, the reason for the noticeable difference of characters between CHF in L-regime and that in H-regime must be attributed to more detailed structure of flow. Discussions on minute structures of flow are beyond the scope of this study of course, but there may be a possibility, for example, to distinguish the CHF ascribed to the dryout of a liquid film on the heated tube wall (L-regime) from the CHF ascribed to the breakdown of a liquid film flow with a finite thickness on the wall (H-regime).

(iv) The result of item (ii) also suggests the possibility that CHF in N-regime is closely related to the so-called DNB (departure from nucleate boiling). In addition, there is an interesting fact that the non-linear $q_c - \Delta H_i$ relationship, constituting a characteristic feature of N-regime, is related to the flow pattern of froth or bubbly flow.

(v) From the results of Figs. 1–3, it may be con-

* $q_{co}/GH_{fg} = 0.25/(l/d)$, which holds in L-regime for $l/d > 100$ and $\sigma\rho_l/G^2l > 7.84 \times 10^{-4}$, is omitted here because it is unnecessary for the range dealt with in this paper.

cluded that CHF does not occur under the condition of slug (or churn) flow.

(vi) Due to the lack of experimental informations of flow pattern for CHF in HP-regime, it is unknown at present whether a new type of flow pattern exists or not for CHF in HP-regime.

5. CONCLUSION

Characteristic regimes of CHF in uniformly heated tubes, determined empirically by the author through the analysis of existing CHF data, are compared with flow regime maps obtained by Bergles and Suo, and by Bennett *et al.*, for the two-phase flow in uniformly heated tubes, clarifying the matters mentioned in items (i) to (vi) of Section 4.

Acknowledgement—I appreciate the financial support to this study offered by the Ministry of Education, Science and Culture [Special Project Research No. 411002 (1979)].

REFERENCES

1. Y. Katto, A generalized correlation of critical heat flux for the forced convection boiling in vertical uniformly heated round tubes, *Int. J. Heat Mass Transfer* **21**, 1527–1542 (1978).
2. Y. Katto, A generalized correlation of critical heat flux for the forced convection boiling in vertical uniformly heated round tubes—a supplementary report, *Int. J. Heat Mass Transfer* **22**, 783–794 (1979).
3. Y. Katto, An analysis of the effect of inlet subcooling on critical heat flux of forced convection boiling in vertical uniformly heated tubes, *Int. J. Heat Mass Transfer* **22**, 1567–1575 (1979).
4. Y. Katto, General features of CHF of forced convection boiling in uniformly heated vertical tubes with zero inlet subcooling, *Int. J. Heat Mass Transfer* **23**, 493–504 (1980).
5. J. C. Collier, *Convective Boiling and Condensation*, p. 238. McGraw-Hill, New York (1972).
6. A. E. Bergles and M. Suo, Investigation of boiling water flow regimes at high pressure, in *Proceedings of the 1966 Heat Transfer and Fluid Mechanics Institute*, pp. 79–99. Stanford University Press, Stanford (1966).
7. A. W. Bennett, G. F. Hewitt, H. A. Kearsey, R. K. F. Keeys and P. M. C. Lacey, Flow visualization studies of boiling at high pressure, *Proc. Instn Mech. Engrs* **180**(3C), 260–270 (1965–66).

SUR LA RELATION ENTRE LE FLUX THERMIQUE CRITIQUE ET LA CONFIGURATION DE L'ECOULEMENT EXTERIEUR POUR L'EBULLITION AVEC CONVECTION FORCEE DANS DES TUBES VERTICAUX ET CHAUFFES UNIFORMEMENT

Résumé — Pour le flux thermique critique (CHF) de l'ébullition avec convection forcée dans des tubes chauffés verticaux, l'auteur a récemment proposé des formules générales classées en quatre régimes CHF caractéristiques appelés *L*, *H*, *N*, et *HP*. Dans ce texte, on étudie la relation entre les régimes précédents et les configurations d'écoulement pour les tubes chauffés uniformément.

EINE BEZIEHUNG ZWISCHEN DER KRITISCHEN WÄRMESTROMDICHTE UND DER STRÖMUNGSFORM AM ROHRAUSTRITT BEIM STRÖMUNGSSIEDEN IN GLEICHMÄSSIG BEHEIZTEN SENKRECHTEN RÖHREN

Zusammenfassung — Zur Berechnung der kritischen Wärmestromdichte beim Strömungssieden in gleichmäßig beheizten senkrechten Rohren hat der Autor in jüngster Zeit allgemeingültige Gleichungen vorgeschlagen. Die Gleichungen gelten für vier charakteristische Bereiche der kritischen Wärmestromdichte, welche L, H, N und HP genannt werden. In der vorliegenden Arbeit wird untersucht, wie die erwähnten Bereiche der kritischen Wärmestromdichte und die Strömungsformen am Rohraustritt zusammenhängen. Dazu werden Angaben über die Strömungsformen bei gleichmäßig beheizten Rohren verwendet.

О СООТНОШЕНИИ МЕЖДУ КРИТИЧЕСКИМ ТЕПЛОВЫМ ПОТОКОМ И КАРТИНОЙ ТЕЧЕНИЯ НА ВЫХОДЕ ИЗ ТРУБЫ ПРИ КИПЕНИИ С ВЫНУЖДЕННОЙ КОНВЕКЦИЕЙ В РАВНОМЕРНО НАГРЕВАЕМЫХ ВЕРТИКАЛЬНЫХ ТРУБАХ

Аннотация — Для критического теплового потока при кипении с вынужденной конвекцией в равномерно нагреваемых вертикальных трубах автором ранее были предложены обобщенные соотношения для четырех характерных режимов критического теплового потока, обозначенных символами *L*, *H*, *N* и *HP*. В данной работе на основании имеющихся данных по характеру течения в равномерно нагреваемых трубах проведено исследование взаимосвязи указанных режимов критического теплового потока и картины течения на выходе из трубы.